

Magnetic Field of Levitated  
Superconducting Quadrupole W VI

F. Rau

IPP 2/67

April 1968

**I N S T I T U T F Ü R P L A S M A P H Y S I K**  
**G A R C H I N G B E I M Ü N C H E N**

INSTITUT FÜR PLASMAPHYSIK

GARCHING BEI MÜNCHEN

April 1968 (in English)

Magnetic Field of Levitated  
Superconducting Quadrupole W VI

F. Rau

Abstract

In part I of this pamphlet we give data of the -up to now-  
final choice of IPP 2/67 configuration of April 1968  
superconducting quadrupole W VI.

In part II we summarize criteria of plasma physical and of  
technical nature used in developing the above configuration.

*Die nachstehende Arbeit wurde im Rahmen des Vertrages zwischen dem Institut für Plasmaphysik GmbH und der Europäischen Atomgemeinschaft über die Zusammenarbeit auf dem Gebiete der Plasmaphysik durchgeführt.*

April 1968 (in English)

Abstract

In part I of this pamphlet we give data of the -up to now-  
final choice of the configuration of the levitated superconduc-  
ting quadrupole W VI.

In part II we summarize criteria of plasma physical and of  
technical nature used in developing the above configuration.

see next page

Part I - Configuration W VI

1. Magnetic Field

We use cylindrical co-ordinates  $R, \varphi, z$ . In a series of computer runs [1] a configuration  $R_n, z_n$  of  $n$  currents  $\vec{I}_n = (0, I_n, 0)$  is derived which produce a magnetic field suitable

- i) to confine [2, 3] a low- $\beta$  plasma in a flute-stable toroidal quadrupole configuration,
- ii) to levitate the two inner rings.

Superimposed to this poloidal field there will be a comparatively weak azimuthal field [2].

In Table I<sup>+</sup> we list the coordinates  $R, z$  of filamentary currents  $I$  and the coordinates  $R, z_1, z_2$  of solenoids having the length  $z_1 - z_2$  and total current  $I$ .

These currents produce a magnetic field as shown in Fig. 1. Field lines (lines of constant vector potential  $AR$ ) are calculated starting at arbitrarily chosen points. Thus equal distance of field lines does not indicate  $B$  proportional to  $R$ . Small crosses show the position of filamentary currents, short vertical straight lines the position of solenoids, dashed lines the contours of the actual coils.

---

+) see next page

J  
30.8  
92.3  
92.3  
92.3  
92.3  
92.3  
63.33  
63.34  
63.33

Table I

Filaments

R	Z	J
24.5	16.0	-17.46
27.5	16.0	-17.46
30.5	16.0	-17.46
33.5	16.0	-17.46
24.5	-16.0	-18.32
27.5	-16.0	-18.32
30.5	-16.0	-18.32
33.5	-16.0	-18.32
57.5	16.0	-16.5
61.5	16.0	-16.5
57.5	-16.0	-18.2
61.5	-16.0	-18.2
70.05	10.05	-12.0
70.05	13.55	-12.0
73.55	10.05	-12.0
73.55	13.55	-12.0
70.05	-10.05	-12.0
70.05	-13.55	-12.0
73.55	-10.05	-12.0
73.55	-13.55	-12.0

Solenoids

R	Z1	Z2	J
27.0	0.7	- 0.7	30.8
28.4	3.4	- 3.4	92.3
29.7	3.4	- 3.4	92.3
31.0	3.4	- 3.4	92.3
32.3	3.4	- 3.4	92.3
61.5	2.1	- 2.1	63.33
60.0	2.1	- 2.1	63.34
58.5	2.1	- 2.1	63.33

We list some properties of this magnetic field configuration

- i) no net flux between the contours of the rings (line  $c_I$  and  $c_{II}$ ), i.e. ring contours are at same vector potential
- ii) difference of vector potential between ring contours  $c_I$  and  $c_{II}$  and separatrix  $s$  equal to difference of vector potential between separatrix and field line  $q_m$  where  $q = \oint dl/B$  is minimum<sup>+</sup>).
- iii) ring contours chosen such as to provide volume for superconducting coils with their structural elements as well as volume for energy storage to ensure the desired time of operation,
- iv) outer boundary field line which is from the line  $q_m$   $\Delta_z = 1.5$  cm distant at  $R = 45.6$  cm. This field line must not be touched by material objects such as cooling device, liquid  $N_2$ -shield etc.,
- v) small asymmetry of magnetic field with respect to plane  $z = 0$  caused by small additional (some %) currents  $I_{ix}, I_{ix}$  in the lower system in order to lift the weight of the rings I and II,
- vi) position of shortest field line (see fig. 3) not optimized,
- vii) no "Rosenbluth-dimple".

In figs. 2 and 3 we plot vector potential  $A_R$  and magnetic field  $B$  as well as volume per unit flux  $q = \oint dl/B$  and length of field line  $L = \oint dl$  as functions of  $R$  at  $z = 0$ .

---

+) These first two criteria imply [2]:

- a) equal particle loss rates to the outer wall and to the surfaces of the levitated rings,
- b) total diamagnetic current equal to zero, no net angular momentum if plasma is produced symmetrical in  $\pm \phi$  direction.

## 2. Magnetic Forces

### a) Equilibrium

In this section we neglect the small overshoot of current in the lower coil system. Magnetic forces are calculated adding the hoop-force  $\vec{K}_h = (K_{h,R}, 0, 0)$ , i.e. force of each current acting on itself, and the force of interaction  $\vec{K}_i = (K_{i,R}, 0, K_{i,z})$  between any current and the magnetic field produced by all the other currents.

#### Hoop force

We assume a coil with total current  $I = nr^2 j_\varphi$ ,  $j_\varphi = \text{const.}$ , forming a toroid of major radius  $R$  and minor radius  $r$ , having the self-inductance  $L \approx \mu_0 R(\ln R/r + 1/3)$  and magnetic energy  $E = -1/2 LI^2$  [4]. The hoop force  $K_h$  is calculated from magnetic energy performing a virtual deformation  $dR$ :

$$K_{h,R} = - \frac{dE}{dR} = - \frac{E}{R} + \mu_0 \frac{I^2}{2} \quad (1)$$

This force is directed radially outward.

Table II gives the hoop forces of the coils of W VI.

Table II

Hoop forces in W VI

coil	R [m]	r [cm]	L [H]	I [A]	E [J]	$K_h$ [Nw]	$K_h$ [kp]
I	0.3	3.75	$0.91 \cdot 10^{-6}$	$4 \cdot 10^5$	$7.3 \cdot 10^4$	$34.3 \cdot 10^4$	$35.0 \cdot 10^3$
II	0.6	2.7	$2.95 \cdot 10^{-6}$	$1.9 \cdot 10^5$	$4.15 \cdot 10^4$	$8.9 \cdot 10^4$	$9.1 \cdot 10^3$
III=IV	0.29	0.35	$1.73 \cdot 10^{-6}$	$7 \cdot 10^4$	$0.43 \cdot 10^4$	$1.8 \cdot 10^4$	$1.8 \cdot 10^3$
V=VI	0.595	0.35	$4.08 \cdot 10^{-6}$	$3.3 \cdot 10^4$	$0.21 \cdot 10^4$	$1.0 \cdot 10^4$	$1.0 \cdot 10^3$
VII=VIII	0.718	0.35	$5.11 \cdot 10^{-6}$	$4.8 \cdot 10^4$	$0.59 \cdot 10^4$	$0.97 \cdot 10^4$	$1.0 \cdot 10^3$

L = self inductance of single-turn coil; coils, having n turns:  
 $I \rightarrow nI$

Force of interaction

The magnetic field  $\vec{B}_i = (B_{ir}, 0, B_{iz})$  as produced by all the other currents at the center of any coil is calculated using the computer-code [1] and skipping the respective current. The force of interaction  $\vec{K}_i$  is given approximately by

$$\vec{K}_i = 2\pi R \vec{I} \times \vec{B}_i = (K_{ir}, 0, K_{iz})$$

as listed in Table III.

Table III

Forces of interaction

coil	I [A]	R [m]	$B_{iz}$ [Vs/m <sup>2</sup> ]	$B_{ir}$	$K_{ir}$ [Nw]	$K_{iz}$ [Nw]	$K_{ir}$ [kp]	$K_{iz}$ [kp]
I	$4 \cdot 10^5$	0.3	+0.04	0	$3 \cdot 10^4$	0	$3.1 \cdot 10^3$	0
II	$1.9 \cdot 10^5$	0.6	-0.21	0	$-1.5 \cdot 10^5$	0	$-15 \cdot 10^3$	0
III=IV	$-7 \cdot 10^4$	0.29	+0.26	0.39	$-3.3 \cdot 10^4$	$+5.0 \cdot 10^4$	$3.4 \cdot 10^3$	$5.1 \cdot 10^3$
V=VI	$-3.3 \cdot 10^4$	0.595	-0.08	0.19	$+1.0 \cdot 10^4$	$+2.3 \cdot 10^4$	$1.0 \cdot 10^3$	$2.3 \cdot 10^3$
VII=VIII	$-4.8 \cdot 10^4$	0.718	-0.09	0.12	$+1.9 \cdot 10^4$	$+2.6 \cdot 10^4$	$1.9 \cdot 10^3$	$2.7 \cdot 10^3$

One of the possible approaches is to calculate the magnetic energy  $E = \frac{1}{2} \sum_{ik} L_{ik} I_i I_k$  as function of relative position of the current hoops and discuss the question of stability considering



Fig. 4 is a graph of the total force  $\vec{K} = \vec{K}_h + \vec{K}_i$ . We note that the inner ring I tends to expand with a total force of  $3.8 \cdot 10^4$  kp whereas the outer ring II is compressed by about  $-6 \cdot 10^3$  kp. The slanting forces acting on the levitating and field-shaping coils can be matched easily by appropriate design of coil supports.

b) Levitation

To levitate the inner rings I and II into the position  $z = 0$  a certain current in the lower coil system  $I_{IX}$  and  $I_X$  added to the current  $I_{IV}$  and  $I_{VI}$  (cf fig. 1) is necessary.

We assume weights of  $G_I = 260$  kg and  $G_{II} = 530$  kg of the levitated rings I and II.

When using the values of vertical forces  $K_{iz}$  of coils III and V (Table III) we find

$$I_{IX} = \frac{G_I}{K_{iz,III}} \cdot I_{III} = \frac{260}{5100} (-7.0 \cdot 10^4) = -3.6 \cdot 10^3 \text{ [A]}$$

$$I_X = \frac{G_{II}}{K_{iz,V}} \cdot I_V = \frac{530}{2300} (-3.3 \cdot 10^4) = -7.6 \cdot 10^3 \text{ [A]}$$

c) Stability

The mechanical stability of current hoops, some of which being levitated, is treated in more detail elsewhere [4, 5, 6].

One of the possible approaches is to calculate the magnetic energy  $E = \frac{1}{2} \sum_{ik} L_{iK} I_i I_K$  as function of relative position of the current hoops and discuss the question of stability considering

- i) whether the energy rises (forces tending to stabilize) or decreases (forces inducing instability) and
- ii) how much the energy changes (frequencies or growth rate, respectively)

when performing a finite displacement off the equilibrium position.

In a system of two levitated movable rings (their shape being unchanged) there exist 10 degrees of freedom [5]. Since in the configuration W VI the currents in the levitated rings are the largest of the whole system, the severest disturbances of equilibrium are considered to be

- i) radial motion of the levitated rings against each other with the same displacement  $\delta_R$
- ii) tilting of the levitated rings about the same angle  $\delta$
- iii) common displacement of the levitated rings in z-direction.

Other displacements are less harmful as the attractive forces of the currents in the levitated rings tend to reduce them.

Keeping all fluxes  $\Phi_i = \sum_K L_{iK} I_K$  constant we calculate for the current distribution of W VI the magnetic energy  $E(\delta_R, \delta)$  at several positions  $z = \text{const}$ . A contour plot  $E(\delta_R, \delta)$ ,  $z = 0$  is given in fig. 5. Solid lines are contours of  $E(\delta_R, \delta) > E(0, 0)$ , and the broken lines those of  $E(\delta_R, \delta) < E(0, 0)$ . The system is stable against tilting, unstable against radial displacement. This radial instability will be servo-controlled [6].

Varying  $z$  similar plots as fig. 5 are found showing only a slight change of the marginal line  $E(\delta_R, \delta) = E(0, 0)$ ;  $Z = \text{const}$ .

In fig. 6 the solid line shows  $E(0, 0)$  as function of  $z$ ; the dashed lines indicate at some positions  $z$   $E(\delta_R, 0)$ , the dotted lines  $E(0, \delta)$ . The system is stable against displacement in  $z$ . As the lower currents are slightly higher than the upper ones the minimum

of the energy is at  $z > 0$ . However, adding the gravitational energy  $E_g = Mgz$  ( $M =$  mass of the two levitated rings) the minimum of energy is shifted to  $z = 0$ , thus defining the overshoot of currents in the lower system once more.

### 3. Change of Magnetic Field and Configuration

Considering particle losses ( $D_d \sim B^{-2}$ ,  $D_B \sim B^{-1}$ ) transverse to magnetic field  $B$  one is interested in changing  $B$  by varying the currents in the system by a factor of  $p$ . As it is desirable to keep the levitated rings floating at position  $z = 0$  one has to change the overshoot in current of the lower system by a factor of  $1/p$  to retain this equilibrium position. In a set of computer runs we changed  $p$  from  $p = 1$  (configuration as in Table I and fig. 1) to  $p = 0.4$  and performed the evaluation of the relevant field lines  $c_I$ ,  $c_{II}$ ,  $s$ ,  $q_m$  (see fig. 1). The dependence of the field configuration is demonstrated in fig. 7. The upper curves in fig. 7 show the relative change

$$\frac{R(p) - R(1)}{R(1)}$$

of typical radii  $R_I$ ,  $R_{II}$ ,  $R_O$ ,  $R_q$  of the ring contours  $c_I$ ,  $c_{II}$ , the separatrix  $s$  and the line with  $q = q_{\min}$ , respectively. For values of  $0.5 \lesssim p \lesssim 1$  these radii deviate less than 1 % and the magnetic flux between separatrix and  $q_{\min}$  (see lower part of fig. 7, constant distance between both curves) is proportional to  $p$ . As the asymmetry of the configuration with respect to  $z = 0$  is aggravated with  $p < 0.5$  and the relevant field lines are shifted

more and more it is concluded that  $0.5 < p < 1$  should be maintained in the experiments. Thus the classical confinement time  $\tau_{cl}$  can be varied by a factor of 4 whereas  $\tau_{Bohm}$  changes by a factor of 2.

## Part II - Criteria Defining the Configuration

Criteria defining the configuration W VI are of plasma physical as well as of technical nature. Strict adherence to one special criterion often leads to contradictory results as compared to the requirements of other criteria. Compromises have to be made which sometimes are influenced by subjective aspects. Furthermore, expected time to realize the project W VI as well as cost considerations are taken into account. Some of these considerations were discussed when the octopole W V was developed [2], others are outlined in prior pamphlets on project W VI [e.g. 7, 8, 9].

### 1. Linear Scaling

Having once chosen a set of currents to be optimal we first consider a linear scaling factor  $k$  which is to be applied to the dimensions of the configuration.

Scaling is done already in [7] and [9]; here we list the assumptions made and the results obtained.

Contrary to the scaling of W V [2] we keep constant

- i) current density of the superconductors
- ii) ion flux produced by the source.

Considering ions of energy  $U$  lost by resistive diffusion or by Bohm-diffusion the respective containment times  $\tau_{cl}$  and  $\tau_B$  are proportional to

$$\tau_d \sim k^{7/2} U^{1/4}, \quad \tau_B \sim k^3 U^{-1}$$

Choosing the number  $n$  of radii of gyration between two field lines, e.g. separatrix and  $q_{\min}$  as a further constant the particle energy  $U$  can be eliminated and one finds

$$\tau_d \sim k^{9/2}, \quad \tau_B \sim k^{-1}$$

This result indicates the choice of maximum possible  $k$ , the upper boundary being given by consideration of costs (e.g. cost of superconducting material  $\sim k^3$ ), of facilities to manufacture the parts and time  $t$  of production ( $t \sim k^2$  to  $k^3$ ), and of having the power already installed to energize the coils.

The discussion of all these points led to dimensions as shown in Table I or fig. 1.

## 2. Currents in the Levitated Rings

Here we give a simple and approximate relation between the total currents in the levitated rings.

We wish to establish no net flux between the two levitated rings 1 and 2, i.e.

$$\Phi_1 \equiv \sum_k L_{1k} I_k = \Phi_2 \equiv \sum_k L_{2k} I_k$$

As the mutual inductances  $L_{1k}$  are always smaller than the self-inductances  $L_{11}$  and as the currents  $I_1, I_2$  are the largest in the configuration we approximate

$$\Phi_1 \approx L_{11} I_1; \quad \Phi_2 \approx L_{22} I_2$$

As the  $L_{11}$  are proportional to the radii  $R_1$  we find  $I_1 R_1 \approx I_2 R_2$ . This first approximation is improved by trial and error. The final result of having no net magnetic flux between the surfaces of the rings is to be in accordance with the demands of the

the superconductors,

following section 4. concerning the cross section of the rings.

### 3. Major Radius of Levitated Rings

Taking the major radius of one ring as given and keeping fluxes constant one can enlarge the major radius of the other ring thus enlarging the plasma volume. We changed the major radius of the bigger of the two levitated rings from  $R_2 = 54.6$  cm (same value as octopole W V) to  $R_2 = 60$  and  $R_2 = 70$  cm. The volume enclosed by the field  $q_m$  was approximately proportional to  $(R_2/R_1 - 1.6)$ , magnetic flux between separatrix and field line  $q_m$  and consequently the particle confinement time was independent of  $R_2/R_1$ . In the case of  $R_2 = 70$  cm there was evidence of flux leaking out in z-direction between the inner and outer levitating coils, and the final choice was  $R_2 = 60$  cm.

### 4. Aspect Ratio of Levitated Rings

The levitated rings consist of superconducting material wound on a rigid frame to meet the magnetic forces, of current switching elements, and of mercury as energy reservoir to ensure appropriate time of operation, all embedded in a vacuum-tight shell.

Considering a possible [10] current density of  $j \approx 10^4$  A/cm<sup>2</sup> for the superconductor corresponding to 200 A in the superconducting tape there result  $n = 2000$  and 950 windings for ring I and II respectively, demanding a cross section of 46 and 22 cm<sup>2</sup> as indicated in fig. 1.

The amount of mercury in the rings depends on

- i) the energy dissipated when energizing the coils,
- ii) the energy dissipated in the normal-conducting switch of the superconductors,

- iii) the thermal energy of plasma lost on the rings,
- iv) the energy radiated onto the surface of the rings.

When discussing these effects one can neglect i) to iii) as compared to iv); an estimate of the power radiated onto the surfaces of the levitated rings ( $N_I$ ,  $N_{II}$  resp.) yields [11] the ratio  $N_I/N_{II} = M_{HgI}/M_{HgII} = 0.46$  in the case of a small spherical plasma source.

## 5. Outer Coils

The outer coils No. III to No. VIII (see fig. 1) are normal-conducting and water cooled. They are switched in series and carry currents in the opposite directions to those of the levitated rings No. I and No. II. The coils IX and X provided for lifting the superconducting rings will be energized separately. Their currents are chosen according to the requirements of the preceding sections 2b and 3 concerning levitation and variation of magnetic field.

When defining the axial position  $z$  of the levitating coils III, IV + IX (corresponding to ring I) and V, VI + X (corresponding to ring II) the currents of those coils are to be proportional to  $z$  to avoid considerable change in the shape of the configuration. An average distance of  $z = 16$  cm is chosen.

The coils No. VII and VIII are necessary to compensate for flux leakage caused by toroidal geometry. They are at a position  $R, z$  such as to introduce no tilting instability on the levitated rings.

Additional to the main poloidal field an azimuthal field  $B_\phi$  of approximately 1 to 2 kG will be provided. This is desirable according to the experimental result of the octopole [12] and also to have the possibility of introducing shear [2].

References

- [1] K.V. v.Hagenow      Fortran-program to calculate axis-  
Y. Kovetz              symmetric-magnetic field (unpublished)
- [2] D.Eckhartt            MPI-PA 6/65  
G. v.Gierke  
G.Grieger
- [3] H.Wobig              Interne Institutsmitteilungen  
IPP No. 5, 1967
- [4] E.Rebhan              Equilibrium and Stability...  
A.Salat                (to be published in Z.f.Naturforschg.)
- [5] H.Wobig              Project W VI, Nov. 1967
- [6] G.Grieger            Dynamic Stabilization...
- [7] G.v.Gierke           Project W VI (13.2.1967)
- [8] F.Rau                Project W VI (14.3.1967)  
J.-G.Wegrowe
- [9] B.Oswald             Project W VI No. 3  
F.Rau  
J.-G.Wegrowe
- [10] B.Oswald            Untersuchung an supraleitfähigen Rin-  
gen (24.4.1967) - unpublished  
and private communication
- [11] F.Rau               Project W VI (February 1968)
- [12] D.Eckhartt          Paper CN 21-50, Culham 1965  
G.v.Gierke  
G.Grieger



Figure Captions

- Fig. 1            Field pattern of superconducting levitated quadrupole W VI
- Fig. 2            Vector potential  $AR$  and magnetic field  $B$  as function of  $R$  at  $z = 0$
- Fig. 3            Volume per unit flux  $q = \oint dl/B$  and length of field lines  $L = \oint dl$  as function of  $R$  at  $z = 0$
- Fig. 4            Radial and axial forces acting on the coils
- Fig. 5            Contour plot of magnetic energy (arbitrary units) vs tilting  $\delta$  and radial displacement  $\delta R$  of the levitated rings
- Fig. 6            Magnetic energy vs elevation  $z$ , fluxes constant  
dashed curves: radial displacement  $\delta_r$   
dotted curves: tilting  $\delta$
- Fig. 7            Effects of change of magnetic field strength by a factor  $p$   
upper curves: relative change of typical radii (see insert)  
lower curves: vector potential of separatrix and of field line with  $q = q_{\min}$

Fig. 1

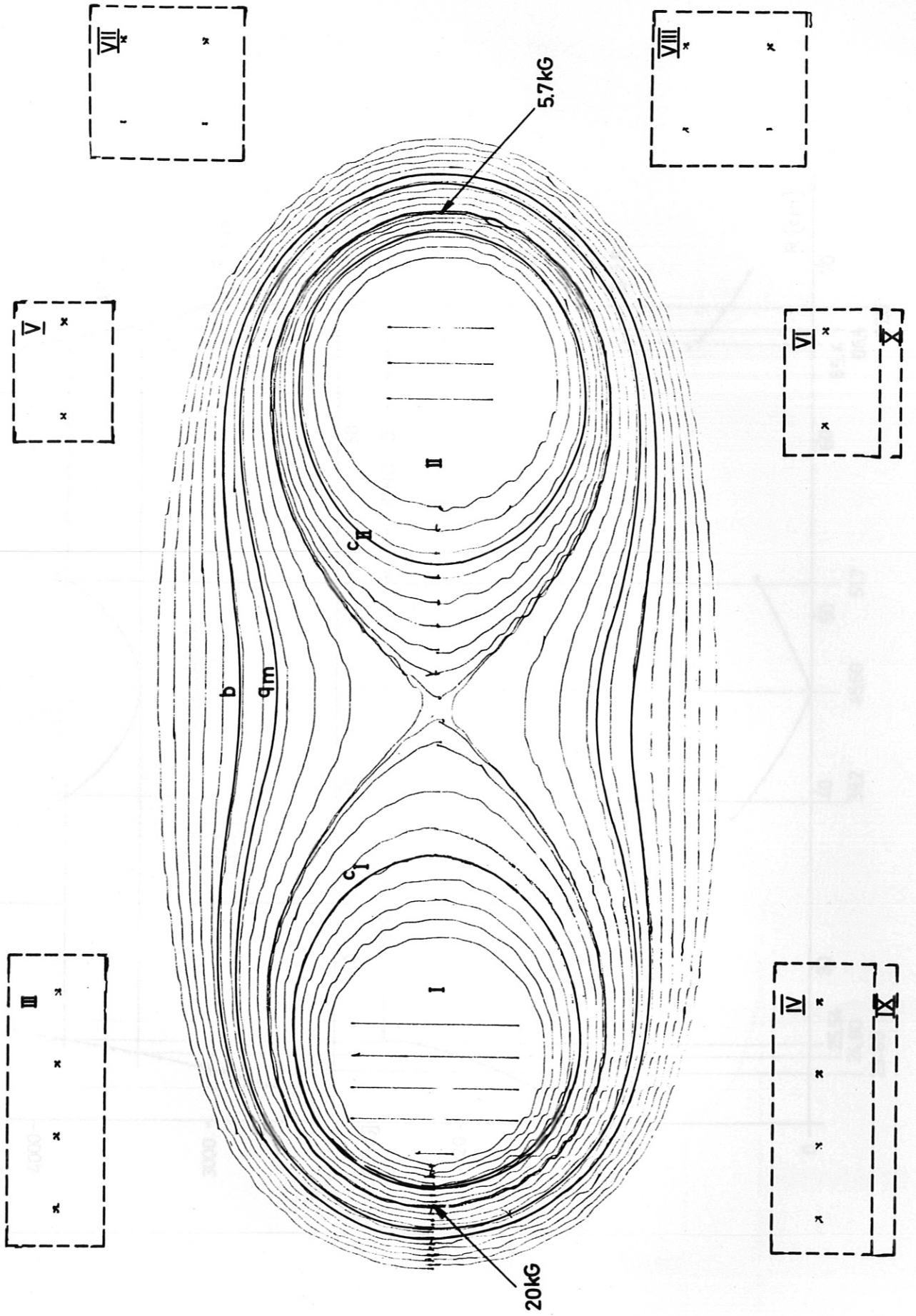


FIG. 2

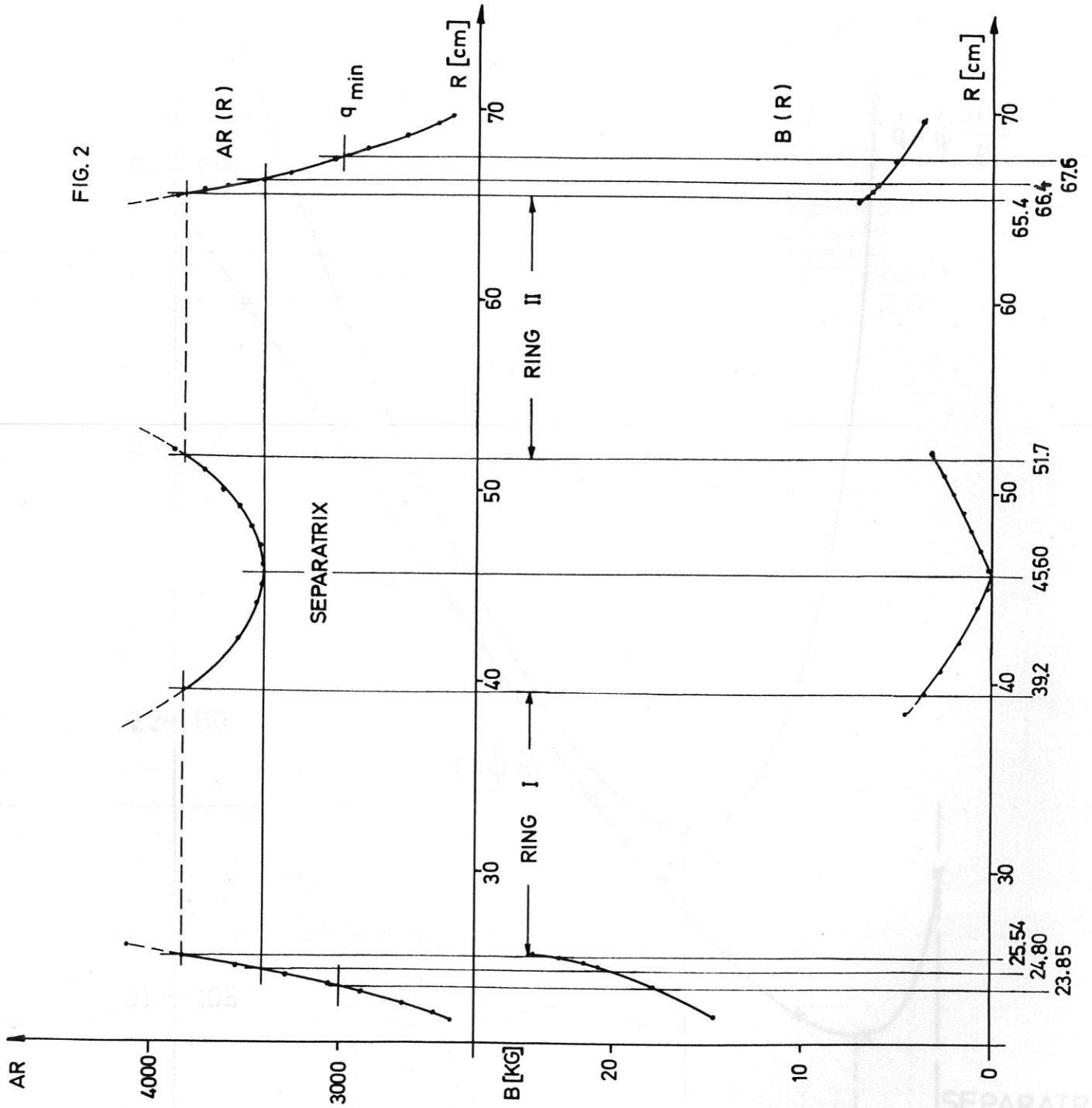
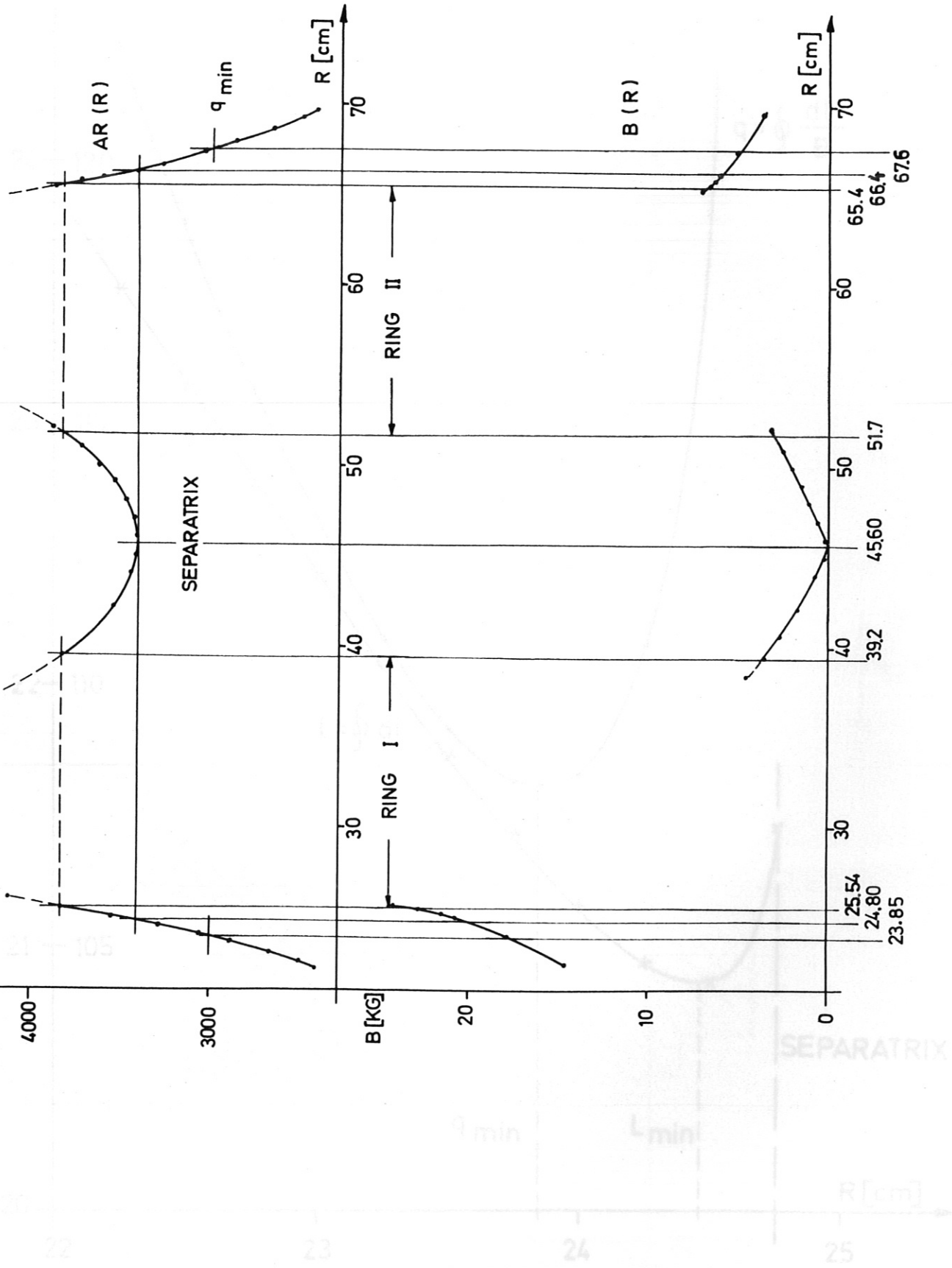


FIG. 3



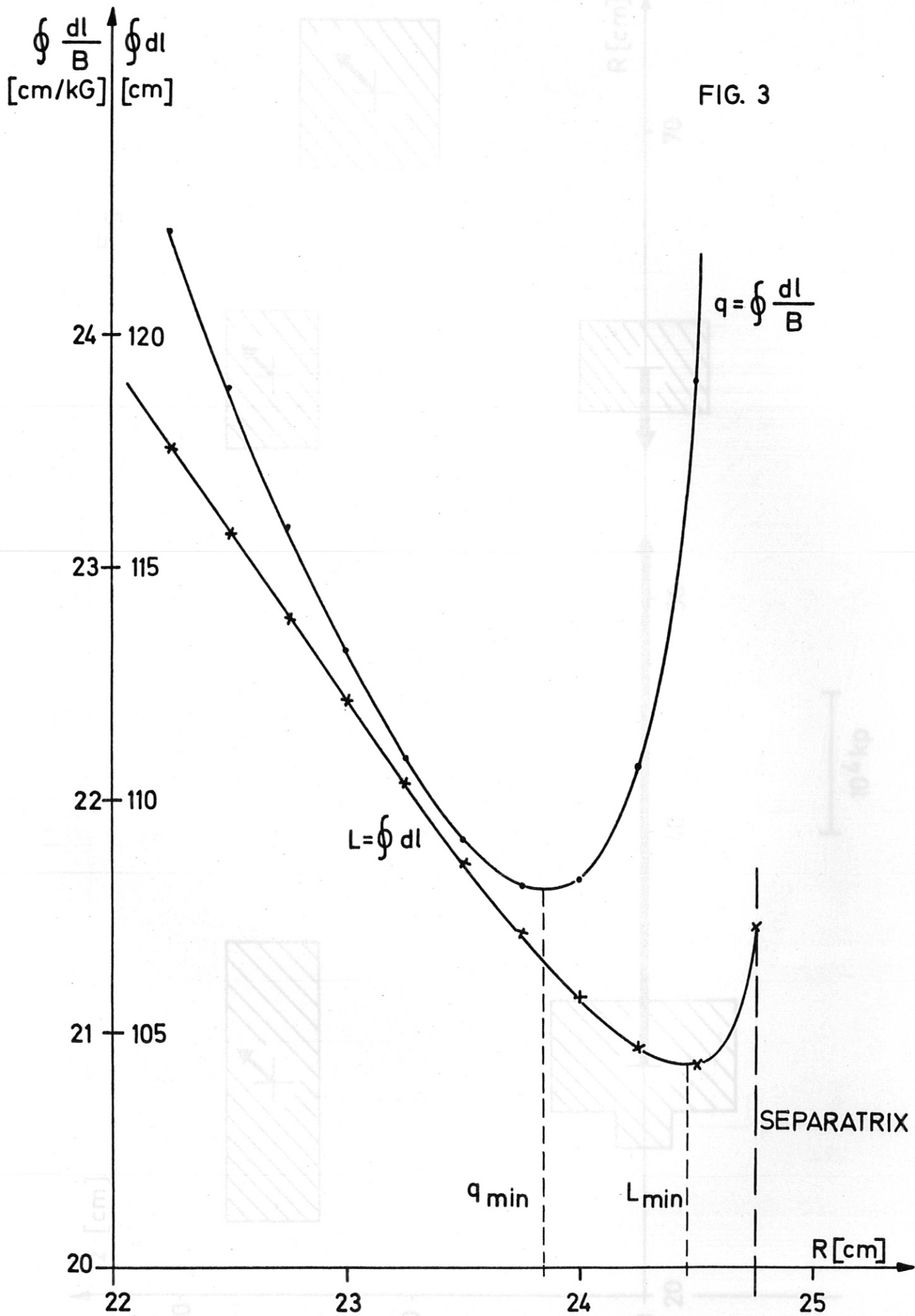


Fig. 4

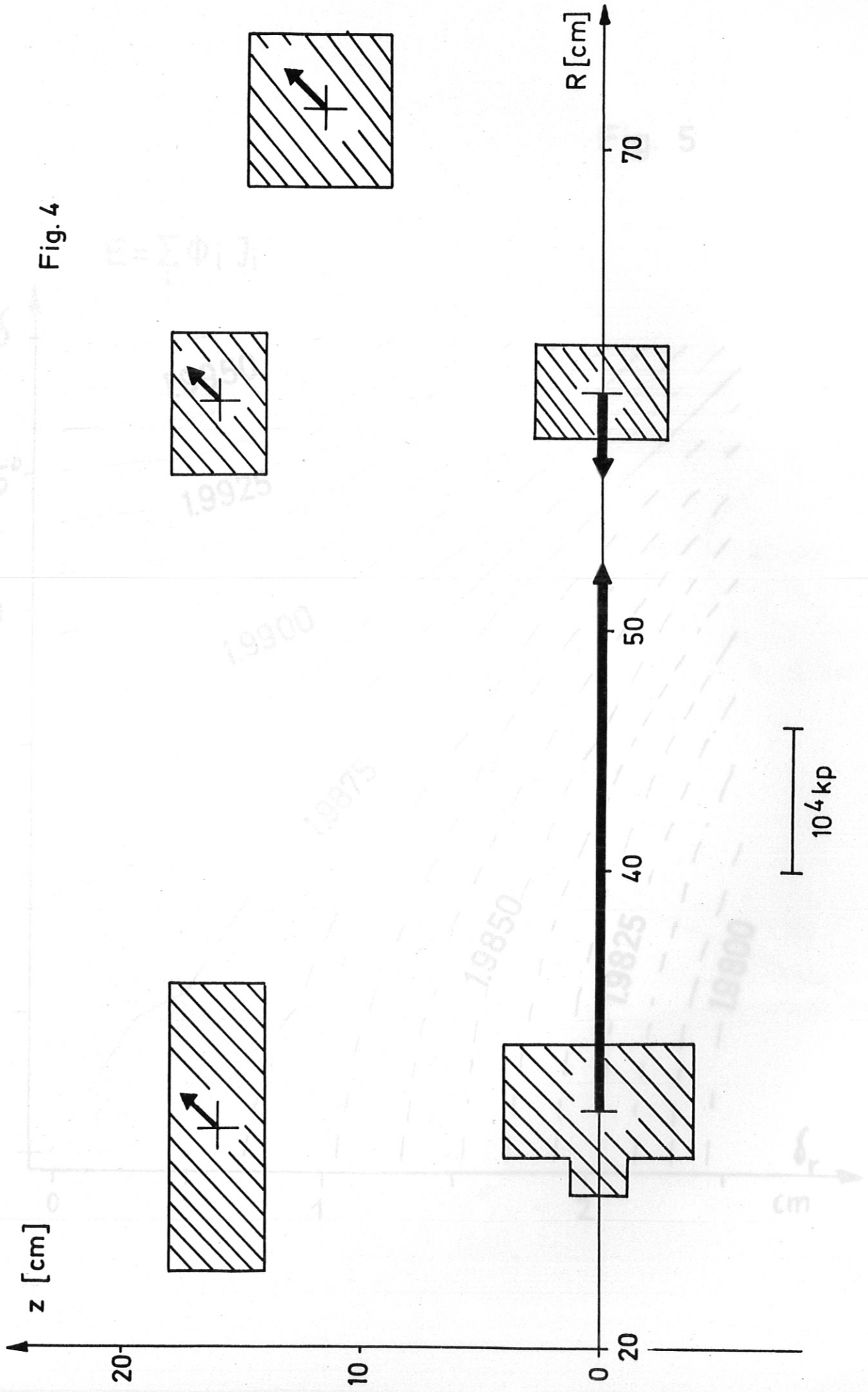


Fig. 5

Fig. 6

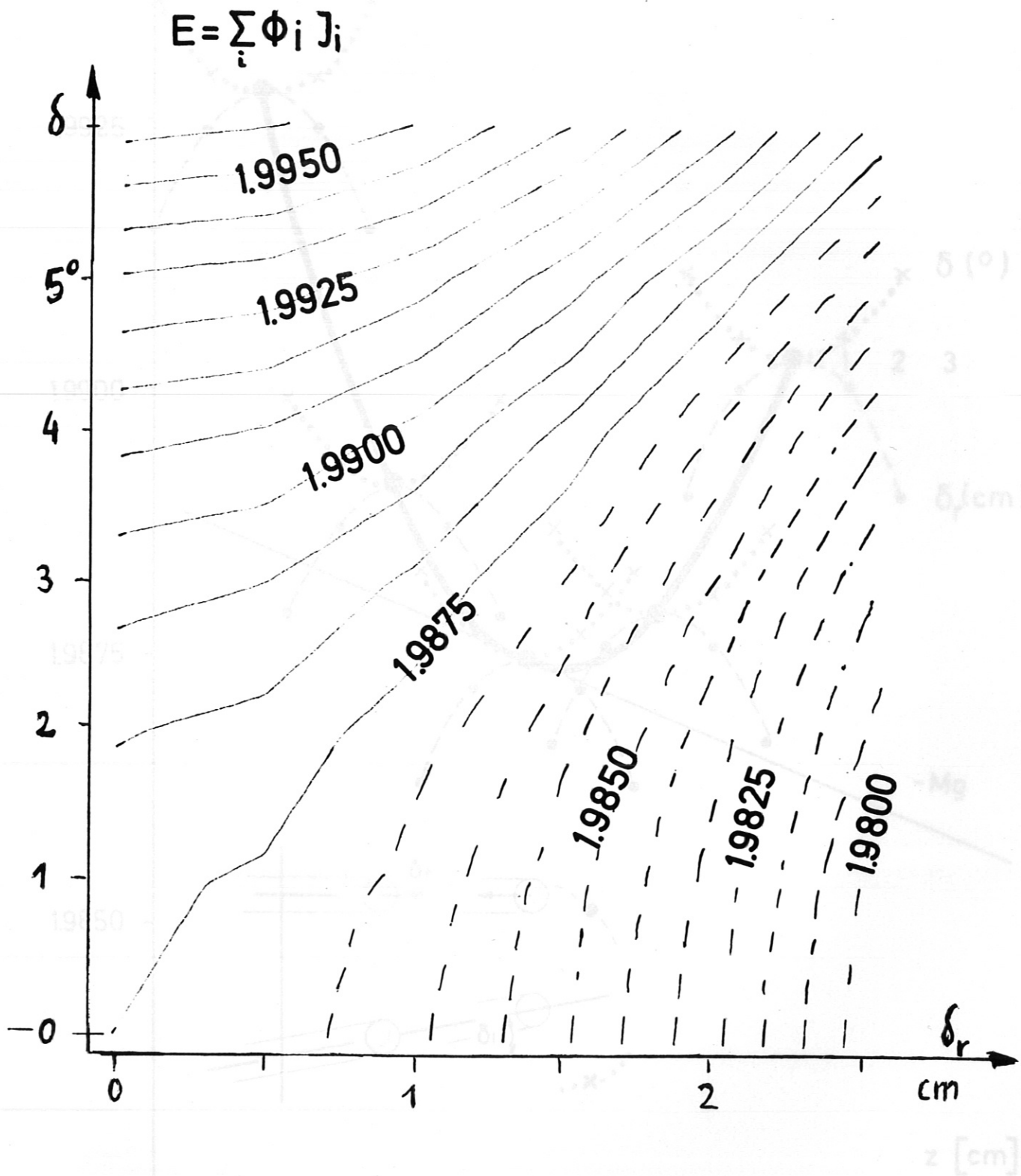


Fig. 6

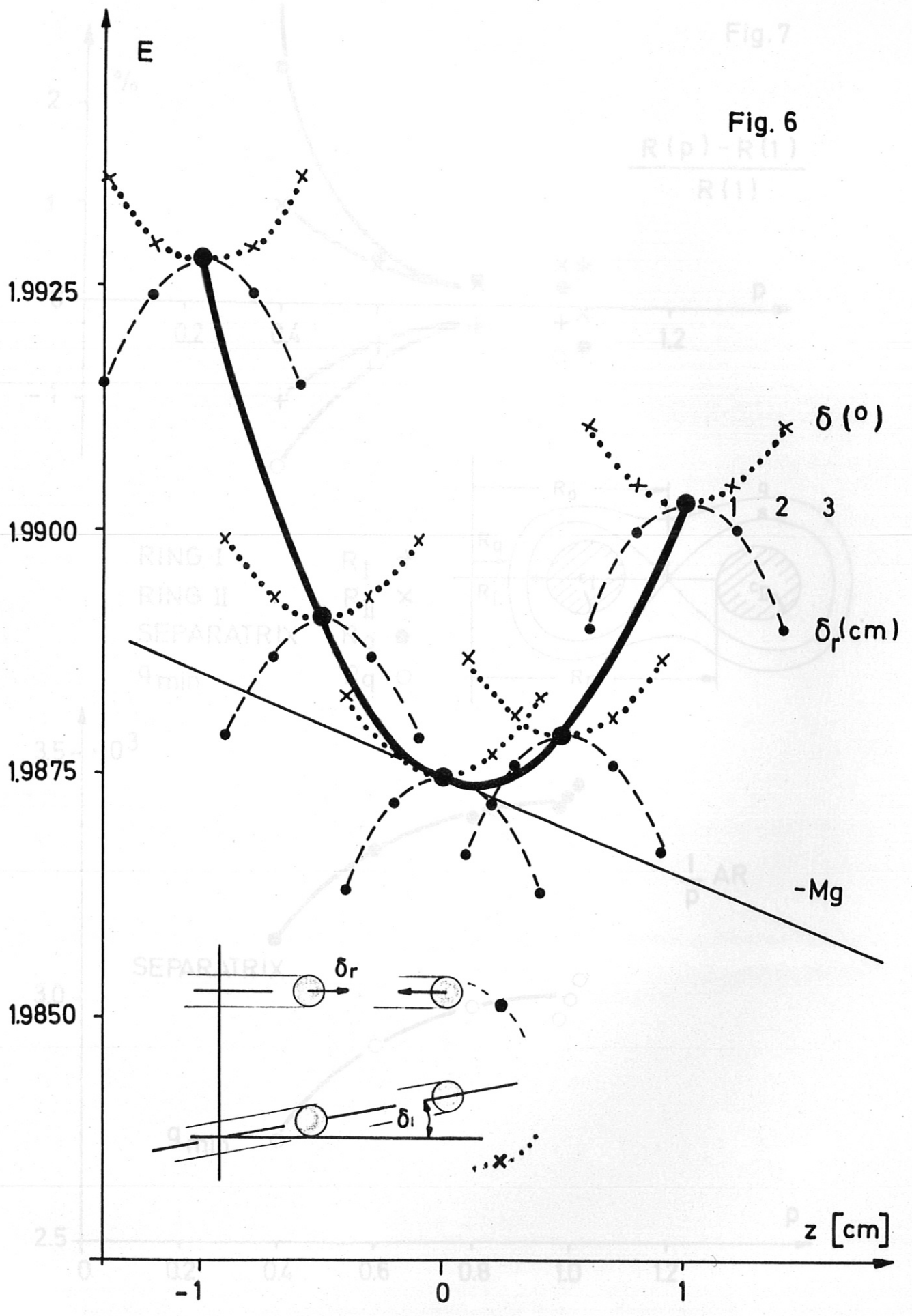
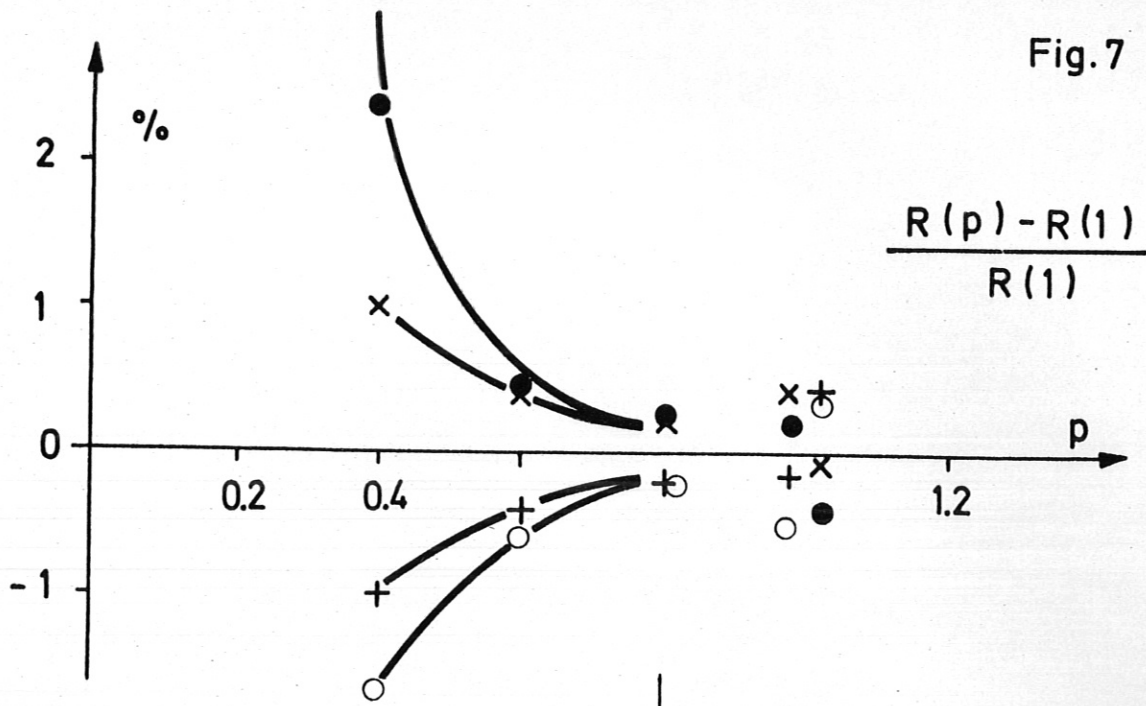


Fig. 7



RING I  
RING II  
SEPARATRIX  
 $q_{min}$

$R_I$  +  
 $R_{II}$  x  
 $R_0$  ●  
 $R_q$  ○

